



DSF-91-10 12/1

DSF-91/19

**SPONTANEOUSLY BROKEN $SU(5)$ SYMMETRIES
AND ONE-LOOP EFFECTS
IN THE EARLY UNIVERSE***

FRANCO BUCCELLA¹, GIAMPIERO ESPOSITO^{2,1} and GENNARO MIELE^{1,2}

⁽¹⁾Dipartimento di Scienze Fisiche, Mostra d'Oltremare Padiglione 19, 80125 Napoli, Italy

⁽²⁾Istituto Nazionale di Fisica Nucleare, Gruppo IV Sezione di Napoli,

Mostra d'Oltremare Padiglione 20, 80125 Napoli, Italy

October 1991

Abstract. This paper studies one-loop effective potential and spontaneous-symmetry-breaking pattern for $SU(5)$ gauge theory in De Sitter space-time. Curvature effects modify the flat-space effective potential by means of a very complicated special function previously derived in the literature. An algebraic technique already developed by the first author to study spontaneous symmetry breaking of $SU(n)$ for renormalizable polynomial potentials is here generalized, for $SU(5)$, to the much harder case of a De Sitter background. A detailed algebraic and numerical analysis provides a better derivation of the stability of the extrema in the maximal subgroups $SU(4) \times U(1)$, $SU(3) \times SU(2) \times U(1)$, $SU(3) \times U(1) \times U(1) \times R_{311}$, $SU(2) \times SU(2) \times U(1) \times U(1) \times R_{2211}$, where R_{311} and R_{2211} discrete symmetries select

particular directions in the corresponding two-dimensional strata. One thus obtains a deeper understanding of the result, previously found with a different numerical analysis, predicting the slide of the inflationary universe into either the $SU(3) \times SU(2) \times U(1)$ or $SU(4) \times U(1)$ extremum. Interestingly, using this approach, one can easily generalize all previous results to a more complete $SU(5)$ tree-level potential also containing cubic terms.

1. Introduction

In the cosmological standard model [1], one assumes that gravity is described by Einstein's general relativity, and that the observed universe is spatially homogeneous and isotropic. Moreover, if the energy-momentum tensor takes a perfect-fluid form, Einstein's equations lead in particular to the following differential equation governing the time evolution of the cosmic scale factor $a(t)$:

$$\left(\frac{\dot{a}}{a}\right)^2 + \frac{k}{a^2} = \frac{8\pi}{3}G\rho \quad , \quad (1.1)$$

where $k = +1, 0, -1$ respectively for a closed, flat or open universe, G is Newton's constant, and ρ is the energy density. In the matter-dominated era ρ is proportional to a^{-3} , and in the radiation-dominated era ρ is proportional to a^{-4} .

The model here outlined, however, leads to a paradox : the universe would contain about 10^{84} regions causally disconnected, although its large-scale properties are described by the Friedmann-Robertson-Walker geometry. Moreover, denoting by ρ_{cr} the energy-density value separating an open from a closed universe, one would find

$$\frac{|\rho - \rho_{cr}|}{\rho} < 10^{-55} \quad . \quad (1.2)$$

This is a severe fine-tuning problem, since condition (1.2) does not seem to arise by virtue of general principles, and appears as an *ad hoc* extra assumption.

However, as shown in [2], one might hope to solve these problems (cf. [3,4]) if the cosmic scale factor $a(t)$ grows exponentially in the early universe, rather than following the

t^γ -behaviour of the cosmological standard model. This can be achieved if the right-hand side of Eq. (1.1) is constant, since this implies

$$a(t) = a_0 \exp\left(\sqrt{\frac{8\pi}{3}} G \rho_0 t\right) \quad , \quad t \in]t_0, t_a[\quad , \quad (1.3)$$

provided the effect of $\frac{k}{a^2}$ can be neglected in the interval $]t_0, t_a[$. One can then show that causally disconnected regions would no longer occur (although severe inhomogeneities can be shown to remain [5]). For this purpose, we need at least a (massive [5,6], or massless self-interacting [7]) scalar field, or a more complete theory of matter fields providing a large vacuum-energy density ($\gg M_W$) which drives *inflation*, i.e. the evolution of $a(t)$ described by Eq. (1.3). If Eq. (1.3) holds, the corresponding geometry is the one of De Sitter space-time, the Lorentzian four-manifold with $R \times S^3$ topology and constant positive scalar curvature.

The naturally occurring candidates for a very fundamental theory which provides at the same time the unification of electro-weak and strong interactions, and a suitably large vacuum energy (see above) for symmetry-breaking are the GUTs [5,8]. Although the minimal $SU(5)$ theory [9] has been ruled out by proton-decay experiments [10,11], the study of this $SU(5)$ model may be very instructive. Moreover, it is worth bearing in mind that $SU(5)$ is contained in $SO(10)$ and E_6 [8].

We here study the one-loop effective potential to determine the phase to which the early universe eventually evolves [12,13]. Since we are interested in quantum-field-theory calculations, we use the Wick-rotated path-integral approach, and we work on the real, Riemannian section of the corresponding complex space-time manifold. Note that this

rotation does not affect the effective potential, while making the perturbative theory well-defined (see below). We are thus interested in the Riemannian version of the De Sitter manifold, with S^4 topology. Its metric is smooth and positive-definite, and the action of the non-abelian Yang-Mills-Higgs theory here studied involves elliptic, self-adjoint, positive-definite differential operators leading to Gaussian integrals, so that the corresponding *one-loop* calculations are well-defined, even though the *full* quantum theory via path integrals does not seem to have rigorous mathematical foundations. Note that we are not quantizing gravity, but we study quantized matter fields in a fixed, curved, Riemannian background geometry via Wick-rotated path integrals and perturbation theory.

Our paper is thus organized as follows. Sect. 2 describes the minimal $SU(5)$ model in De Sitter space and the corresponding results for the one-loop effective potential [13]. Sect. 3 presents the basic results about the tree-level Higgs potential for $SU(5)$ gauge theory in flat space [14]. The special function \mathcal{A} occurring in the corresponding one-loop calculation in a De Sitter background is then studied in detail. Sect. 4 provides the generalization of the technique used in [14] to a De Sitter background. Absolute minima are derived using both analytic and numerical calculations, improving the understanding obtained in [13]. Exact, approximate and asymptotic formulae for the one-loop effective potential are shown to shed new light on the $SU(5)$ symmetry-breaking pattern. Finally, the concluding remarks are presented in Sect. 5.

2. $SU(5)$ model in De Sitter space

Following the introduction and [13], the bare Lagrangian \mathcal{L}_0 and the renormalizable tree potential of our $SU(5)$ Yang-Mills-Higgs theory in De Sitter space are taken to be respectively (after analytic continuation to the Riemannian manifold with S^4 topology)

$$\mathcal{L}_0 = \frac{1}{4} \text{Tr}(\mathbf{F}_{\mu\nu} \mathbf{F}^{\mu\nu}) + \frac{1}{2} \text{Tr} \left[(D_\mu \Phi) (D^\mu \Phi)^\dagger \right] + V_0(\Phi) \quad , \quad (2.1)$$

$$V_0(\Phi) = \frac{\xi}{2} R \text{Tr}(\Phi^2) + \Lambda_2 (\text{Tr} \Phi^2)^2 + \Lambda_4 (\text{Tr} \Phi^4) \quad , \quad (2.2)$$

where $\mathbf{F}_{\mu\nu} \equiv \nabla_\mu \mathbf{A}_\nu - \nabla_\nu \mathbf{A}_\mu - ig[\mathbf{A}_\mu, \mathbf{A}_\nu]$, and $D_\mu \Phi \equiv \partial_\mu \Phi - ig[\mathbf{A}_\mu, \Phi]$. Note that the covariant derivative ∇_μ differs from ∂_μ for terms involving Christoffel symbols [1], and $V_0(\Phi)$ is assumed to obey the symmetry $V_0(\Phi) = V_0(-\Phi)$. Moreover, as usual, g is the dimensionless coupling constant and $R = \frac{12}{r^2}$ is the scalar curvature of De Sitter space (r being the four-sphere radius).

The Higgs scalar field Φ is assumed to be in the adjoint representation of $SU(5)$ [13]. The presence in the minimal $SU(5)$ model of an additional representation (5) of scalar fields \mathbf{H} , necessary to break the symmetry down to $SU(3)_C \times U(1)_Q$, is irrelevant for the inflationary scheme, due to the smaller mass value $M_H \approx M_W$.

The background-field method is now applied to obtain the one-loop form of the potential, writing the Higgs field as $\Phi_0 + \tilde{\Phi}$, where Φ_0 is a constant background field and $\tilde{\Phi}$

a fluctuation around Φ_0 (and similarly for \mathbf{A}^μ). As explained in [13], it is convenient to choose t'Hooft's gauge-fixing term

$$\mathcal{L}_{G.F.} = \frac{\alpha}{2} \text{Tr} \left(\nabla_\mu \mathbf{A}^\mu - ig\alpha^{-1} [\Phi_0, \Phi] \right)^2, \quad (2.3)$$

and Coleman-Weinberg's theory can be used to neglect the contribution of all scalar-field loop diagrams. This implies that only gauge-field loop diagrams are relevant. A very convenient form of the one-loop potential is obtained using the gauge invariance of the theory which enables one to diagonalize the scalar field Φ . The corresponding diagonal form of Φ is here denoted by $\hat{\Phi} = \text{diag}(\varphi_1, \varphi_2, \varphi_3, \varphi_4, \varphi_5)$, where $\sum_{i=1}^5 \varphi_i = 0$. Thus, denoting by $\psi(t)$ the special function $\frac{\Gamma'(t)}{\Gamma(t)}$, and defining

$$\begin{aligned} \mathcal{A}(z) \equiv & \frac{z^2}{4} + \frac{z}{3} - \int_2^{\frac{3}{2} + \sqrt{\frac{1}{4} - z}} t \left(t - \frac{3}{2} \right) (t - 3) \psi(t) dt \\ & - \int_1^{\frac{3}{2} - \sqrt{\frac{1}{4} - z}} t \left(t - \frac{3}{2} \right) (t - 3) \psi(t) dt, \end{aligned} \quad (2.4)$$

the one-loop effective potential for the minimal SU(5) model is found to be [13]

$$\begin{aligned} V(\hat{\Phi}) = & \frac{15}{64\pi^2} \left\{ Q + \frac{1}{3} \left(1 - \log(r^2 M_X^2) \right) \right\} R g^2 \| \hat{\Phi} \| \\ & + \left\{ \frac{9}{128\pi^2} \left(1 - \log(r^2 M_X^2) \right) - \frac{21}{320\pi^2} \Lambda \right\} g^4 \| \hat{\Phi} \|^2 \\ & + \frac{15}{128\pi^2} \left\{ \frac{12}{5} \Lambda + \left(1 - \log(r^2 M_X^2) \right) \right\} g^4 \sum_{i=1}^5 \varphi_i^4 \\ & - \frac{3}{16\pi^2 r^4} \sum_{i,j=1}^5 \mathcal{A} \left[\frac{r^2 g^2}{2} (\varphi_i - \varphi_j)^2 \right], \end{aligned} \quad (2.5)$$

where [13]

$$Q \equiv \frac{32\pi^2}{15g^2} \left[\xi - \frac{8}{5g^2} \left(\Lambda_2 + \frac{7}{30} \Lambda_4 \right) \right] \quad , \quad (2.6)$$

$$\Lambda \equiv \frac{64\pi^2}{15g^4} \left(\frac{3}{5} \Lambda_4 - \Lambda_2 \right) \quad , \quad (2.7)$$

$$\| \Phi \|^2 \equiv \sum_{i=1}^5 \varphi_i^2 \quad , \quad (2.8)$$

and M_X is related to the dimensional parameter μ appearing in the (regularized) one-loop amplitudes [12]. Moreover, if $\xi = \frac{1}{6}$, the Higgs field is conformally coupled to gravity.

The one-loop potential $V(\hat{\Phi})$ is then used to determine broken-symmetry phases and curved-space phase diagrams as shown in [13]. As a result of his numerical analysis, the author of [13] found what follows :

(1) In the $SU(5)$ theory, the universe, in addition to the right $SU(3) \times SU(2) \times U(1)$ direction, is also likely to end up in the wrong $SU(4) \times U(1)$ phase;

(2) The $SU(2) \times SU(2) \times U(1) \times U(1) \times R_{2211}$ and $SU(3) \times U(1) \times U(1) \times R_{311}$ phases are unstable for any values of the parameters appearing in the model.

As we said in the introduction, the aim of this paper is to provide a better understanding of the results obtained in [13]. For this purpose, we recall some basic results about spontaneous symmetry breaking of $SU(n)$ [14], and about the \mathcal{A} function [13] defined in Eq. (2.4).

3. Polynomial potentials and the \mathcal{A} function

To study the spontaneous-symmetry-breaking directions of the potential in Eq. (2.5), it is convenient to define the variables

$$a_i \equiv \frac{g r}{\sqrt{2}} \varphi_i \quad . \quad (3.1)$$

For our purpose, it is not strictly needed to study the part of the potential depending on the norm of the \mathbf{a} field : $\|\mathbf{a}\| \equiv \sum_{i=1}^5 a_i^2$. The relevant part of the potential is instead given by (up to the multiplicative constant $\frac{3r^{-4}}{16\pi^2}$)

$$V_M \equiv b \sum_{i=1}^5 a_i^4 - \sum_{i,j=1}^5 \mathcal{A}[(a_i - a_j)^2] \quad , \quad (3.2)$$

$$b \equiv 6\Lambda + \frac{5}{2} \left(1 - \log(r^2 M_X^2) \right) \quad . \quad (3.3)$$

As a first step, it is useful to recall the exact results [14] holding for a theory where V_M is only given by the first term on the right-hand side of Eq. (3.2). In that case, since $\sum_{i=1}^5 a_i$ is set to zero, and $\sum_{i=1}^5 a_i^2$ equals $\|\mathbf{a}\|$ by definition, the Lagrange-multipliers technique can be used to study the third-order algebraic equations leading to the calculation of the minima [14].

The corresponding results yield, for the minima with the residual symmetry :

$$\mathbf{a} = a_{321} \equiv \frac{\|\mathbf{a}\|^{\frac{1}{2}}}{\sqrt{30}} \text{diag}(2, 2, 2, -3, -3) \quad , \quad (SU(3) \times SU(2) \times U(1)) \quad , \quad (3.4)$$

$$\mathbf{a} = a_{2211} \equiv \frac{\|\mathbf{a}\|^{\frac{1}{2}}}{2} \text{diag}(1, 1, 0, -1, -1) , \quad (SU(2) \times SU(2) \times U(1) \times U(1) \times R_{2211}) , \quad (3.5)$$

$$\mathbf{a} = a_{311} \equiv \frac{\|\mathbf{a}\|^{\frac{1}{2}}}{\sqrt{2}} \text{diag}(0, 0, 0, 1, -1) , \quad (SU(3) \times U(1) \times U(1) \times R_{311}) , \quad (3.6)$$

$$\mathbf{a} = a_{41} \equiv \frac{\|\mathbf{a}\|^{\frac{1}{2}}}{\sqrt{20}} \text{diag}(1, 1, 1, 1, -4) , \quad (SU(4) \times U(1)) , \quad (3.7)$$

the hierarchy

$$V_M(a_{41}) > V_M(a_{311}) > V_M(a_{2211}) > V_M(a_{321}) \quad (3.8)$$

if $b > 0$, and the reversed inequalities if $b < 0$. Thus, when the Higgs field is in the adjoint representation, the $SU(5)$ symmetry breaking leads only to the $SU(4) \times U(1)$ or $SU(3) \times SU(2) \times U(1)$ symmetric minima.

Since the complete V_M potential is in our case given by Eqs. (3.2-3), we need to study in detail the contribution of the \mathcal{A} function. While performing this analysis, it is useful to supplement definition (2.4) by the Taylor expansion of \mathcal{A} as $z \rightarrow 0$, and its asymptotic expansion as $z \rightarrow \infty$, which are given respectively by [13]

$$\begin{aligned} \mathcal{A}(z) = & 2 \left(\gamma - \frac{1}{3} \right) z + \frac{(\gamma - 1)}{2} z^2 + \frac{z^3}{6} \left(-5 + 4\zeta(3) \right) \\ & + \frac{z^4}{24} \left(-36 + 30\zeta(3) \right) + O(z^5) , \end{aligned} \quad (3.9)$$

$$\mathcal{A}(z) \sim - \left(\frac{z^2}{4} + z + \frac{19}{30} \right) \log(z) + \frac{3}{8} z^2 + z , \quad (3.10)$$

where γ is Euler's constant and ζ is the Riemann zeta-function [12]. Using Eqs. (2.4) and (3.9-10), we have found inequalities analogous to (3.8). In other words, defining

$$\mathcal{A}(a_{41}) \equiv - \sum_{i,j=1}^5 \mathcal{A}[(a_i - a_j)^2]_{\mathbf{a}=a_{41}} \quad , \quad (3.11)$$

and similarly for the other phases, one finds

$$\mathcal{A}(a_{41}) > \mathcal{A}(a_{311}) > \mathcal{A}(a_{2211}) > \mathcal{A}(a_{321}) \quad , \quad (3.12)$$

where

$$\begin{aligned} \mathcal{A}(a_{41}) &= -8\mathcal{A}\left(\frac{5}{4}\|\mathbf{a}\|\right) \quad , \\ \mathcal{A}(a_{311}) &= -12\mathcal{A}\left(\frac{\|\mathbf{a}\|}{2}\right) - 2\mathcal{A}(2\|\mathbf{a}\|) \quad , \\ \mathcal{A}(a_{2211}) &= -8\mathcal{A}\left(\frac{\|\mathbf{a}\|}{4}\right) - 8\mathcal{A}(\|\mathbf{a}\|) \quad , \\ \mathcal{A}(a_{321}) &= -12\mathcal{A}\left(\frac{5}{6}\|\mathbf{a}\|\right) \quad . \end{aligned} \quad (3.13, 14, 15, 16)$$

The inequalities appearing in Eq. (3.12) are illustrated in Figures 1-3.

4. Absolute minima

For fixed values of the bare parameters $\xi, \Lambda_2, \Lambda_4$ and M_X (cf. Eqs. (2.6,7) and (3.3)), b depends on r as shown in Eq. (3.3). Thus in the early universe, at small values of r , i.e.

when the scalar curvature is very large, b is positive, whereas it may become negative as r increases.

As shown in Sect. 3, when $b > 0$, the two terms of the V_M potential in Eq. (3.2) follow the inequalities (3.8) and (3.12). This implies that in the very early universe the only possible phase transition is $SU(5) \rightarrow SU(3) \times SU(2) \times U(1)$.

By contrast, for suitably large values of r , b becomes negative, and the polynomial part of the V_M potential is then dominant. In this case the analysis in [14] holds, and the phase transition occurs in the $SU(4) \times U(1)$ direction (i.e. the previous hierarchy is inverted).

A more detailed analysis is however in order when $b < 0$ but $|b|$ is not too large. For this purpose, using the Taylor expansion (3.9) up to third-order, we begin by studying the range of validity of the inequalities

$$V_M(a_{41}) > V_M(a_{311}) > V_M(a_{2211}) > V_M(a_{321}) \quad . \quad (4.1)$$

Thus, defining $\Omega \equiv \frac{(-5+4\zeta(3))}{6} < 0$, one finds

$$\left[V_M(a_{41}) - V_M(a_{321}) \right] > 0 \iff 12b + 60(1 - \gamma) > -250 |\Omega| \| \mathbf{a} \| \quad , \quad (4.2)$$

$$\left[V_M(a_{311}) - V_M(a_{321}) \right] > 0 \iff 12b + 60(1 - \gamma) > -475 |\Omega| \| \mathbf{a} \| \quad , \quad (4.3)$$

$$\left[V_M(a_{2211}) - V_M(a_{321}) \right] > 0 \iff 12b + 60(1 - \gamma) > -850 |\Omega| \| \mathbf{a} \| \quad , \quad (4.4)$$

$$\left[V_M(a_{41}) - V_M(a_{311}) \right] > 0 \iff 12b + 60(1 - \gamma) > 150 |\Omega| \| \mathbf{a} \| \quad , \quad (4.5)$$

$$\left[V_M(a_{41}) - V_M(a_{2211}) \right] > 0 \iff 12b + 60(1 - \gamma) > -225 |\Omega| \| \mathbf{a} \| \quad , \quad (4.6)$$

$$\left[V_M(a_{311}) - V_M(a_{2211}) \right] > 0 \iff 12b + 60(1 - \gamma) > -450 |\Omega| \| \mathbf{a} \| \quad . \quad (4.7)$$

In light of Eqs. (4.2)-(4.7), if Eq. (4.5) is satisfied, this ensures that all remaining conditions hold. One thus obtains the inequality

$$b > 5(\gamma - 1) + \left[\frac{25}{2} |\Omega| \| \mathbf{a} \| + O(\| \mathbf{a} \|^2) \right] = b_0 \quad , \quad (4.8)$$

which is a necessary and sufficient condition for the validity of Eq. (4.1) when the Taylor expansion (3.9) is a good approximation. Note that the term in square brackets on the r.h.s. of Eq. (4.8) is a small correction of the value $5(\gamma - 1) < 0$ provided $\| \mathbf{a} \| \rightarrow 0$, as one would expect when the Taylor expansion makes sense. Interestingly, the inequalities (4.1) still hold for negative values of b provided Eq. (4.8) is satisfied, whereas the flat-space tree-level potential $\hat{V}_M = \hat{b} \sum_{i=1}^5 a_i^4$ used in [14] leads to the value $b_0 = 0$.

Moreover, the reversed hierarchy (cf. (4.1))

$$V_M(a_{321}) > V_M(a_{2211}) > V_M(a_{311}) > V_M(a_{41}) \quad (4.9)$$

holds provided the following necessary and sufficient condition is satisfied (cf. (4.4)) :

$$b < 5(\gamma - 1) + \left[-\frac{425}{6} |\Omega| \| \mathbf{a} \| + O(\| \mathbf{a} \|^2) \right] = b_1 \quad . \quad (4.10)$$

Again, the De Sitter background leads to a value $b_1 \neq 0$ with respect to the flat-space tree-level-potential result $b_1 = b_0 = 0$.

This preliminary analysis should be supplemented by a more detailed numerical study. The aim of this investigation is to prove that, for *all* values of $\| \mathbf{a} \|$ and b , the phase

transition occurs only in the $SU(3) \times SU(2) \times U(1)$ or $SU(4) \times U(1)$ directions. From our previous discussion (see also Figures 4-6), when $b \rightarrow +\infty$ the absolute minimum is in the $SU(3) \times SU(2) \times U(1)$ direction. However, if we compute for fixed $\| \mathbf{a} \|$ the negative $\bar{b}^0, \bar{b}^1, \bar{b}^2$ values of b such that

$$V_M(\bar{b}^0, a_{321}) = V_M(\bar{b}^0, a_{41}) \quad , \quad (4.11)$$

$$V_M(\bar{b}^1, a_{321}) = V_M(\bar{b}^1, a_{2211}) \quad , \quad (4.12)$$

$$V_M(\bar{b}^2, a_{321}) = V_M(\bar{b}^2, a_{311}) \quad , \quad (4.13)$$

we find $\bar{b}^0 > \bar{b}^1$ and $\bar{b}^0 > \bar{b}^2, \forall \| \mathbf{a} \|$. This means that the continuous transition to (4.9) leads to the interchanging of the $SU(3) \times SU(2) \times U(1)$ with the $SU(4) \times U(1)$ absolute minimum. Of course, similar interchanges also occur for the relative minima, but they do not affect the phase transition of the universe.

Defining

$$V_M^{(P)} \equiv \sum_{i=1}^5 a_i^4 \quad , \quad (4.14)$$

and using Eqs. (3.13)-(3.16), it is useful to bear in mind the formulae for \bar{b}^0, \bar{b}^1 and \bar{b}^2 obtained from Eqs. (4.11)-(4.13) :

$$\bar{b}^0 = \frac{[\mathcal{A}(a_{321}) - \mathcal{A}(a_{41})]}{[V_M^{(P)}(a_{41}) - V_M^{(P)}(a_{321})]} \quad , \quad (4.15)$$

$$\bar{b}^{-1} = \frac{[\mathcal{A}(a_{321}) - \mathcal{A}(a_{2211})]}{[V_M^{(P)}(a_{2211}) - V_M^{(P)}(a_{321})]} \quad , \quad (4.16)$$

$$\bar{b}^{-2} = \frac{[\mathcal{A}(a_{321}) - \mathcal{A}(a_{311})]}{[V_M^{(P)}(a_{311}) - V_M^{(P)}(a_{321})]} \quad . \quad (4.17)$$

The differences $(\bar{b}^0 - \bar{b}^{-1})$ and $(\bar{b}^0 - \bar{b}^{-2})$ are plotted in Figures 4-6 as functions of $\| \mathbf{a} \|^{1/2}$ using Eqs. (4.15)-(4.17).

5. Concluding remarks

This paper has shown that the results in [14] about the $SU(n)$ symmetry breaking in flat space may be generalized to a curved, cosmological background such as De Sitter space.

The results in [13] have been thus re-obtained, by virtue of the properties of the \mathcal{A} function (Eq. (2.4) and Figures 1-3). They confirm that the absolute minimum of the complete one-loop potential lies either in the $SU(3) \times SU(2) \times U(1)$ or in the $SU(4) \times U(1)$ direction. This provides a better understanding (cf. [13]) of the instability of the $SU(3) \times U(1) \times U(1) \times R_{311}$ and $SU(2) \times SU(2) \times U(1) \times U(1) \times R_{2211}$ extrema, since very simple and basic algebraic and numerical techniques have been used (cf. Sect. 4).

Interestingly, we can extend all our results to the most general and renormalizable tree-level potential also containing cubic terms, since the tree-level potential does not affect the one-loop contribution within the Coleman-Weinberg approach [12,13,15], and

the presence of an additional cubic term in $V_M^{(P)}$ (see (4.14)) favours the directions a_{41} and a_{321} (for which $V_M^{(P)} < 1$) with respect to a_{311} and a_{2211} (for which $V_M^{(P)} = 0$). The $SU(n)$ symmetry-breaking pattern for this more general class of potentials in flat space can be found in [16], where the author extends and confirms the results obtained in [14]. The approach considered above might be used to discuss the general case of arbitrary directions in the adjoint representation of $SU(5)$; one expects, however, that even in this more general case the absolute minimum will be in the directions found by limiting the analysis to the one-dimensional orbits.

The method here described may be applied to other GUT theories, e.g. with $SO(10)$ or E_6 gauge groups, in De Sitter space [13]. These models appear as more realistic candidates for a unified theory of non-gravitational interactions [8]. One would then obtain a physically more relevant application of the techniques used in this paper.

References

- [1] Weinberg S 1972 *Gravitation and Cosmology* (New York : John Wiley and Sons)
- [2] Guth A H 1981 *Phys. Rev. D* **23** 347
- [3] Ellis G F R and Stoeger W 1988 *Class. Quantum Grav.* **5** 207
- [4] Padmanabhan T and Seshadri T R 1988 *Class. Quantum Grav.* **5** 221
- [5] Linde A D 1984 *Rep. Progr. Phys.* **47** 925
- [6] Hawking S W 1984 *Nucl. Phys. B* **239** 257
- [7] Esposito G and Platania G 1988 *Class. Quantum Grav.* **5** 937
- [8] O’Raifeartaigh L 1986 *Group Structure of Gauge Theories* (Cambridge : Cambridge University Press)
- [9] Georgi H and Glashow S L 1974 *Phys. Rev. Lett.* **32** 438
- [10] Becker-Szendy R et al. 1990 *Phys. Rev. D* **42** 2974
- [11] Buccella F, Miele G, Rosa L, Santorelli P and Tuzi T 1989 *Phys. Lett. B* **233** 178
- [12] Allen B 1983 *Nucl. Phys. B* **226** 228
- [13] Allen B 1985 *Ann. Phys.* **161** 152
- [14] Buccella F, Ruegg H and Savoy C A 1980 *Nucl. Phys. B* **169** 68.
- [15] Coleman S and Weinberg E 1973 *Phys. Rev. D* **7** 1888
- [16] Ruegg H 1980 *Phys. Rev. D* **22** 2040

Figure captions

Figure 1. Differences of \mathcal{A} values corresponding to (a) full curve $[\mathcal{A}(a_{41}) - \mathcal{A}(a_{321})]$, (b) broken curve $[\mathcal{A}(a_{311}) - \mathcal{A}(a_{321})]$ and (c) dotted curve $[\mathcal{A}(a_{2211}) - \mathcal{A}(a_{321})]$. They are evaluated using the Taylor expansion (3.9).

Figure 2. Differences of logarithms₁₀ of \mathcal{A} values corresponding to

- (a) full curve $\log_{10} [\mathcal{A}(a_{41})/\mathcal{A}(a_{321})]$,
- (b) broken curve $\log_{10} [\mathcal{A}(a_{311})/\mathcal{A}(a_{321})]$ and
- (c) dotted curve $\log_{10} [\mathcal{A}(a_{2211})/\mathcal{A}(a_{321})]$.

They are obtained using the exact formula (2.4) defining $\mathcal{A}(z)$.

Figure 3. Differences of logarithms₁₀ of \mathcal{A} values corresponding to

- (a) full curve $\log_{10} [\mathcal{A}(a_{41})/\mathcal{A}(a_{321})]$,
- (b) broken curve $\log_{10} [\mathcal{A}(a_{311})/\mathcal{A}(a_{321})]$ and
- (c) dotted curve $\log_{10} [\mathcal{A}(a_{2211})/\mathcal{A}(a_{321})]$.

The asymptotic expansion (3.10) is here applied.

Figure 4. The dotted curve corresponds to the difference $(\bar{b}^0 - \bar{b}^1)$, and the full curve corresponds to the difference $(\bar{b}^0 - \bar{b}^2)$, where \bar{b}^0 , \bar{b}^1 and \bar{b}^2 have been obtained in Eqs. (4.15)-(4.17). The Taylor expansion (3.9) is here used for $\mathcal{A}(z)$.

Figure 5. Dotted and full curve have the same meaning as in Figure 4. The exact formula (2.4) is here used for $\mathcal{A}(z)$.

Figure 6. Dotted and full curve are defined as in Figures 4 and 5. The asymptotic expansion (3.10) of $\mathcal{A}(z)$ is here applied.

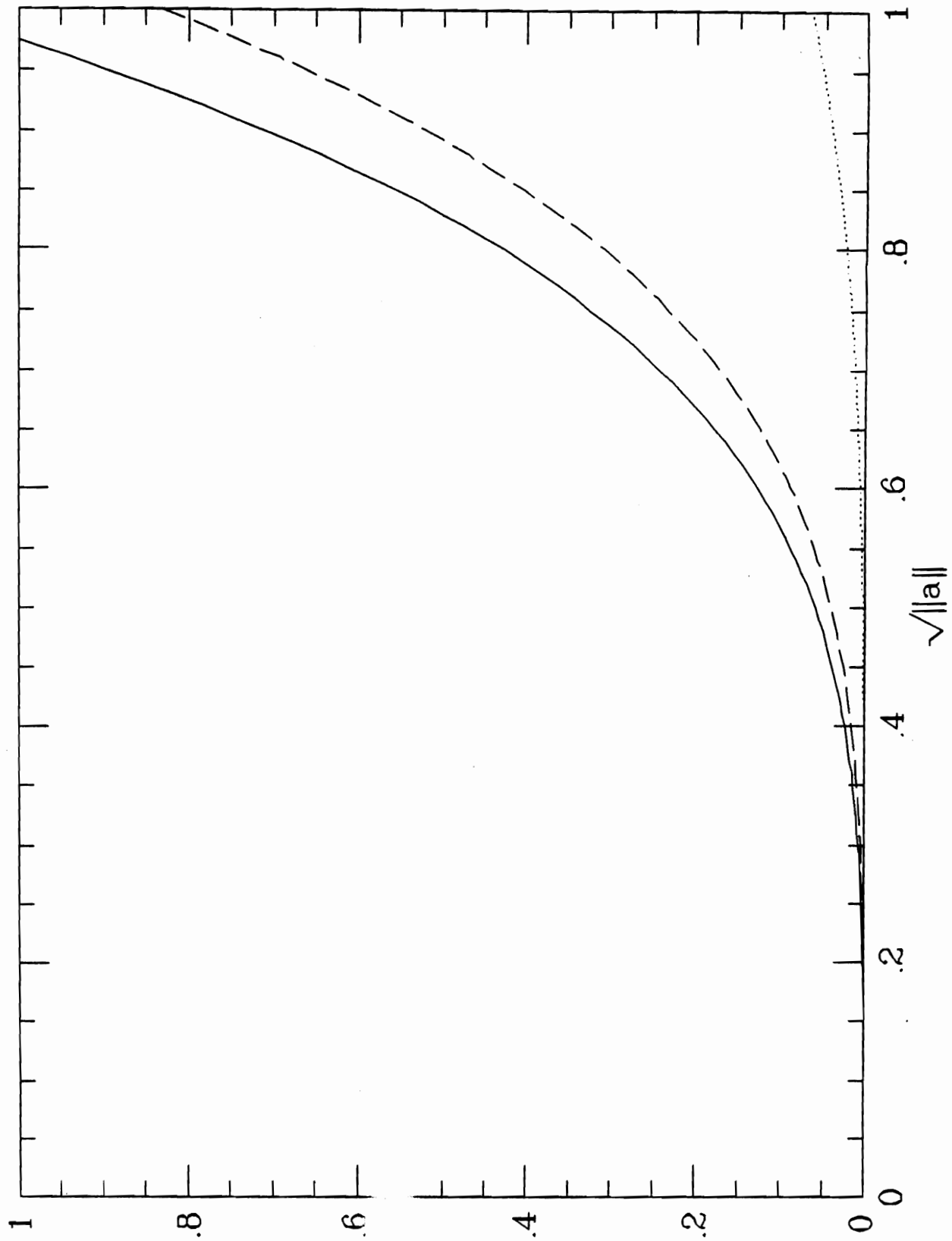


Fig. 1.

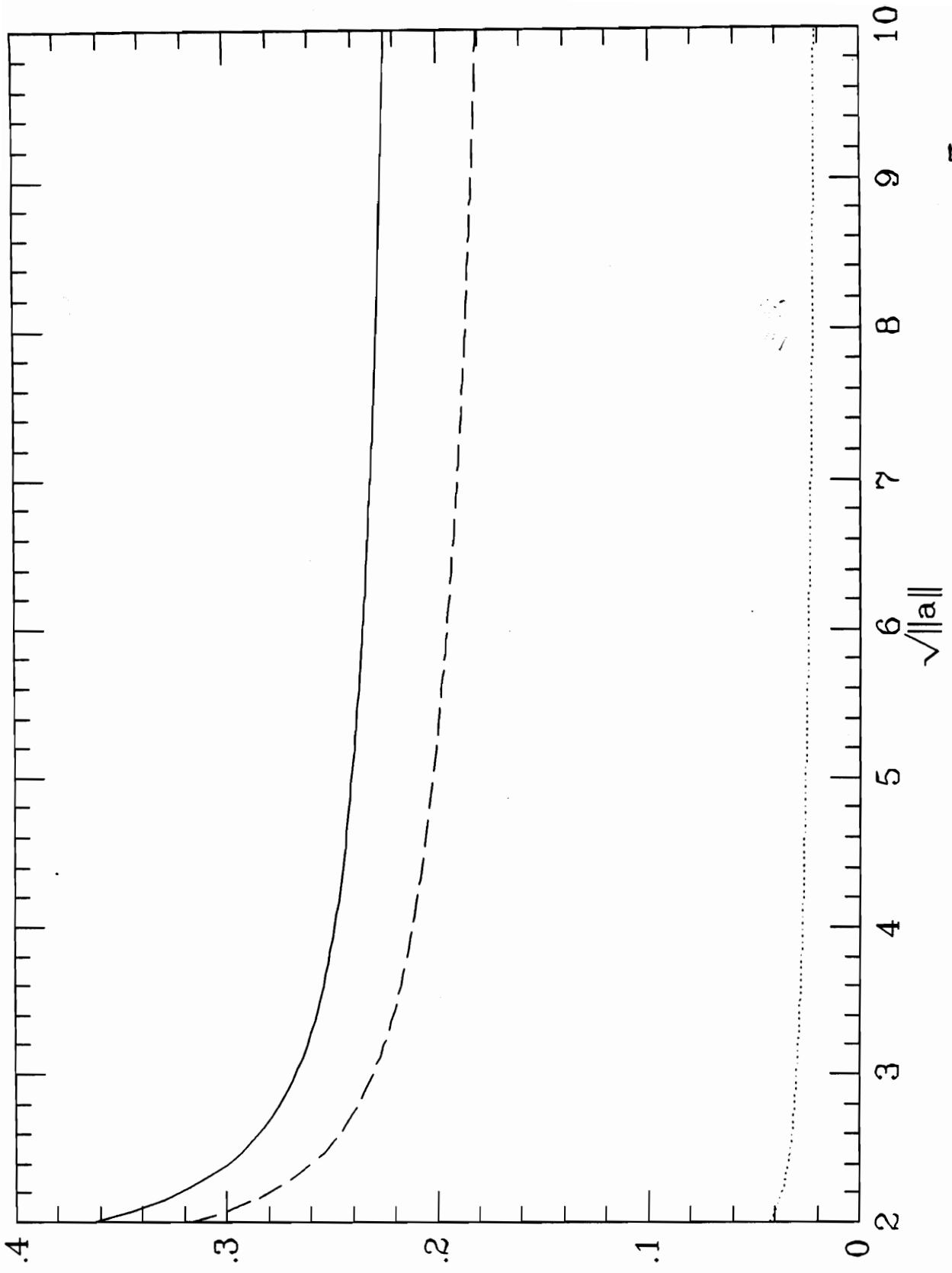


Fig. 2.

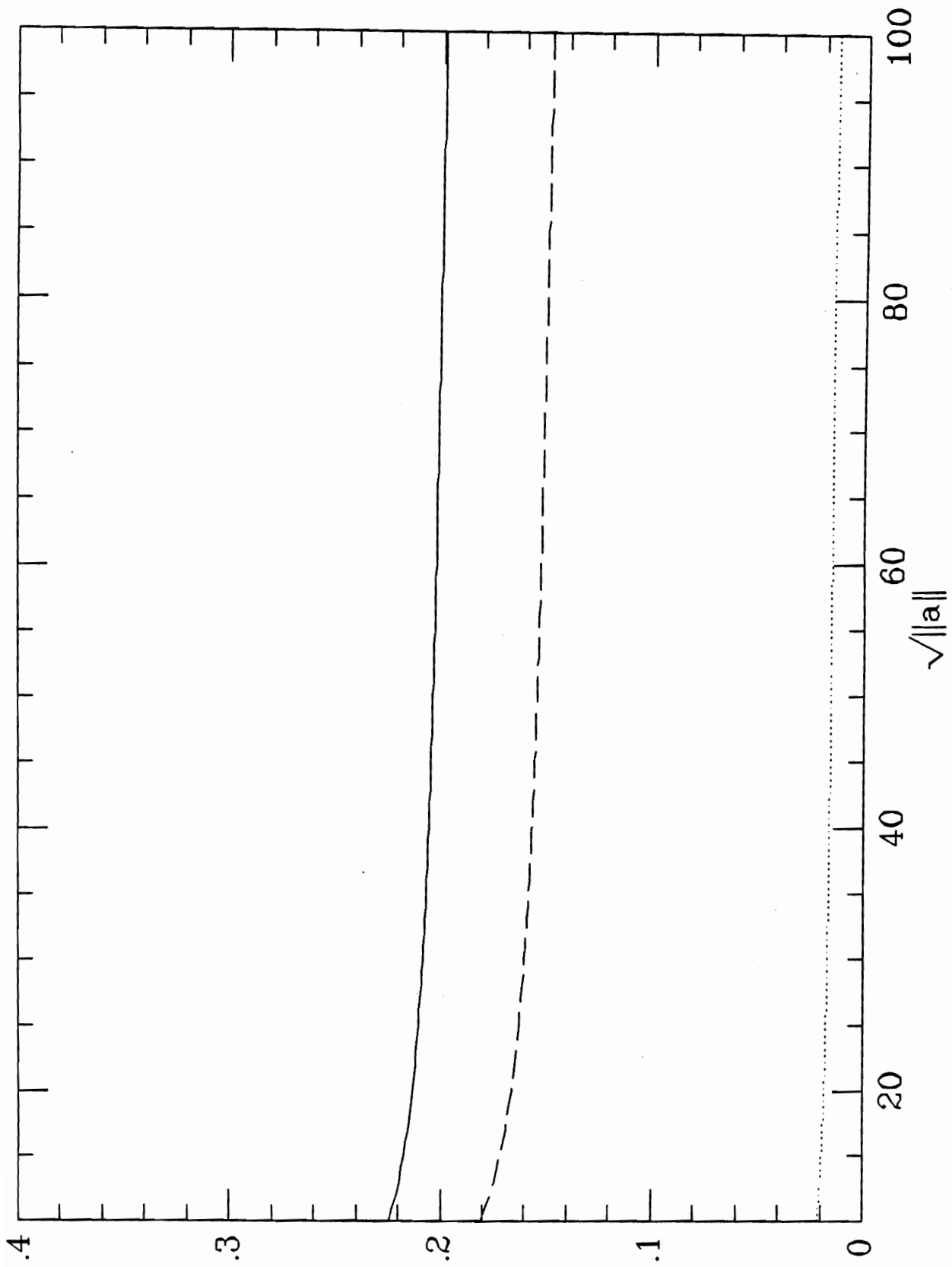


Fig. 3.

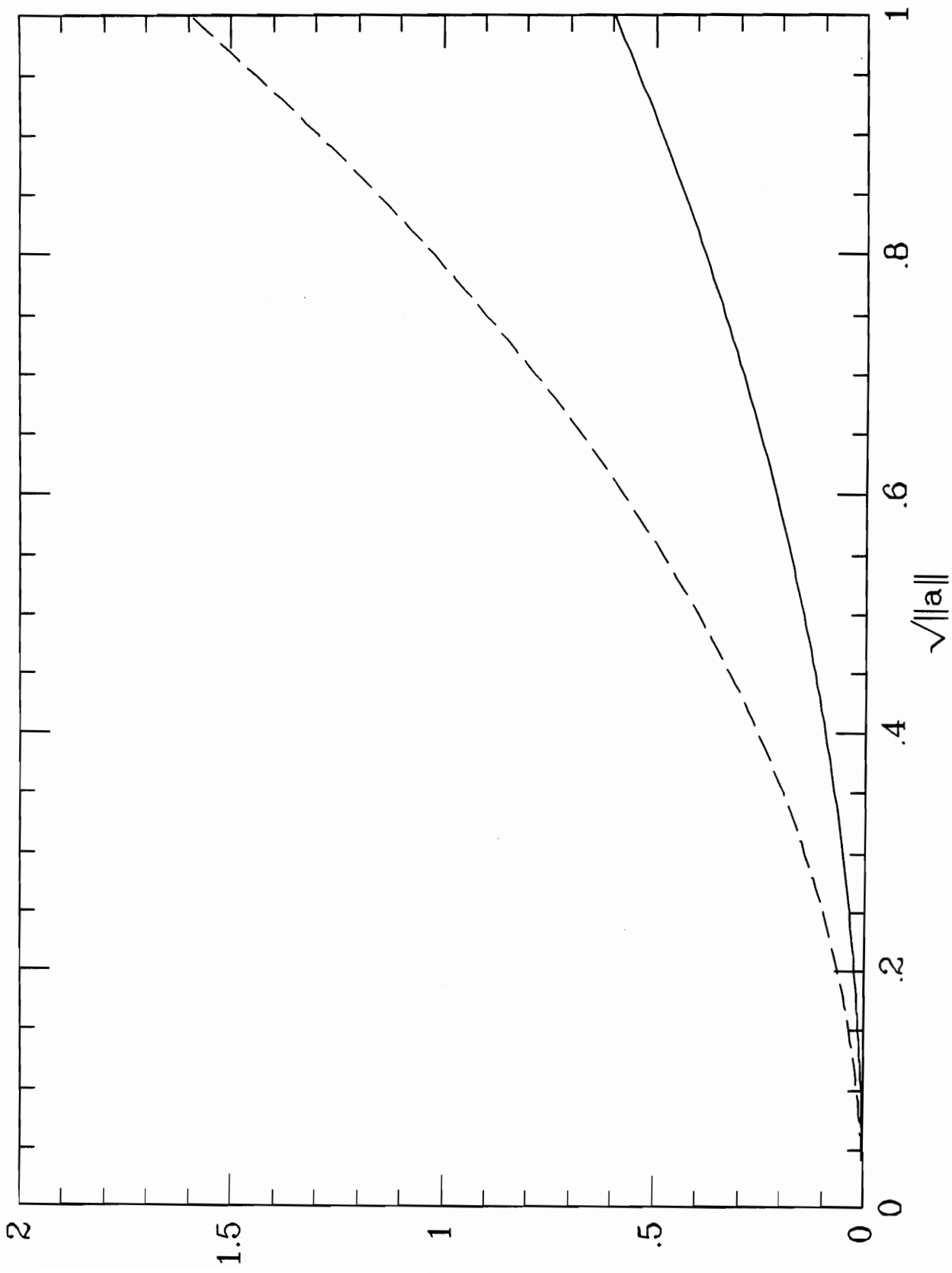


Fig. 4.

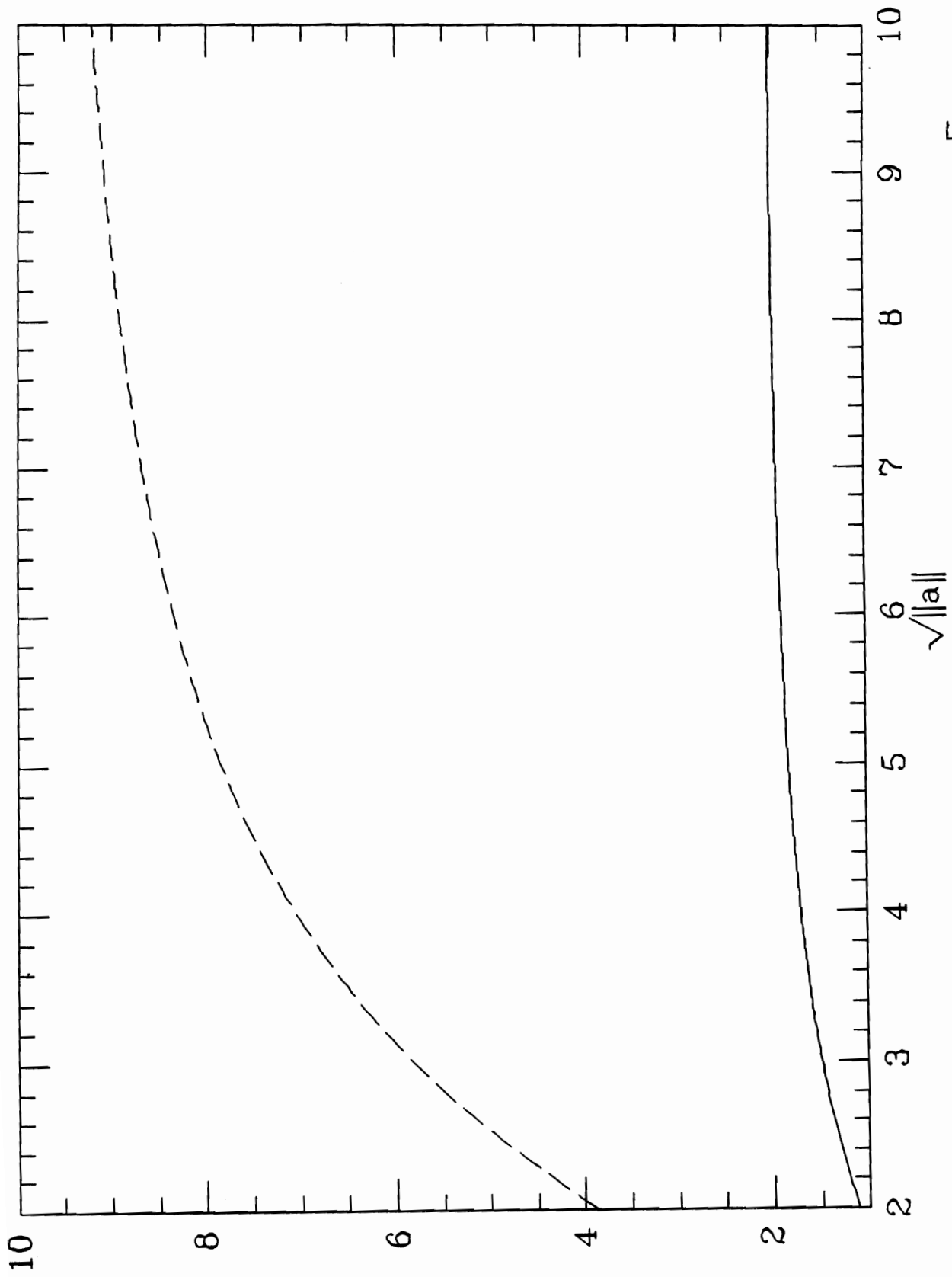


Fig. 5.

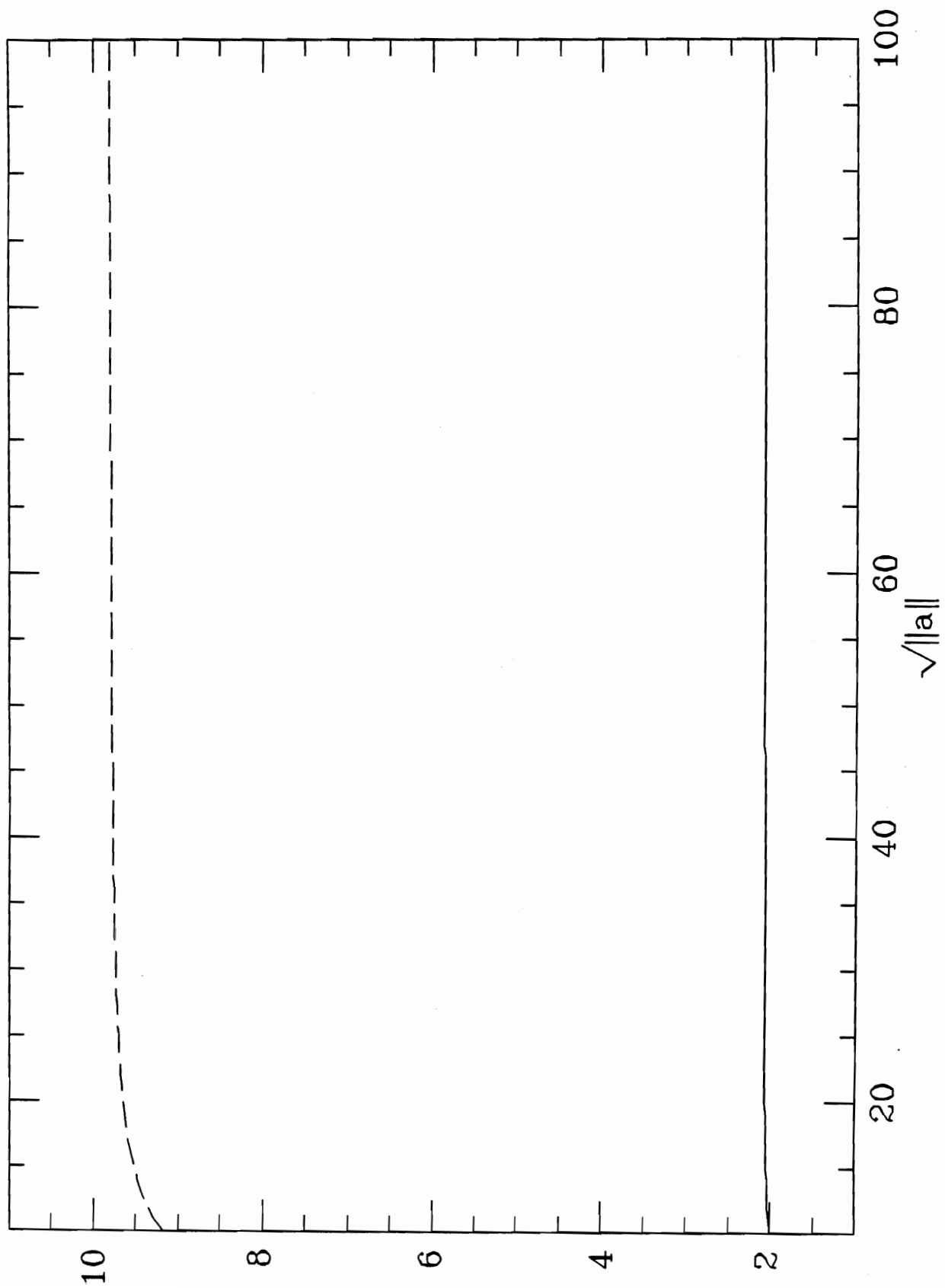


Fig. 6.